



HYDROCHEMICAL CHARACTERISTICS OF GROUNDWATER AND MULTIVARIATE STATISTICAL ANALYSIS ALONG THE COASTAL REGIONS OF PONNERI AND TIRUVOTRIYUR TALUKS OF THIRUVALLUR DISTRICT, TAMIL NADU

Ravikumar P^{1.}, Chandrasekar V^{2.}, Imrana Banu F^{2.}, Shaik Mahamad^{1.}, and Bhaskaran G^{3.}

¹ Department of Geography, Presidency College (A), Chennai

² Department of Geography, Government Arts College for Women, Nilakottai, Dindigul

³ Department of Geography, University of Madras, Guindy, Chennai

Corresponding Author: ravikumarpalaniswamy@gmail.com

Abstract

Groundwater depletion in the Ponneri and Tiruvotriyur coastal regions is worsening due to population growth, urbanization, and industrialization, notably by Ennore Port and Thermal Power Plant. This study is carried out by collecting 37 groundwater samples from open and bore wells during pre-monsoon and post-monsoon seasons indicating high levels of EC, pH, TDS, Na⁺, and Cl⁻, rendering 51% of wells are unfit for drinking, and has adversely impacted agricultural production. The multivariate statistical analysis in R has confirmed the saltwater intrusion. The spatial distribution of major ions of groundwater samples are clearly shows the flow of ground water from Southeast to West and Northwest.

Keywords: Groundwater, Coastal Area, GIS, R Language, and Statistical Analysis

Introduction

In India, there has been a significant upsurge in the demand for groundwater, propelled by rapid population growth, intensified industrialization, and urbanization (Prasad B., et.al 2021). Groundwater is the primary water source for drinking, agriculture, and industry, particularly in arid and semi-arid regions. (N Adimalla et al., 2020). Only 0.3% of the world's freshwater is readily available on the surface, such as in rivers, lakes, and reservoirs, while groundwater constitutes 30% of the freshwater reserve (Nitasha Khatri et al., 2014). It is crucial to recognize that nearly 44% of the global population resides within 150 kilometers of coastlines (Atlas, 2010), placing significant pressure on coastal aquifer systems, which are vital resources for human needs (Bachaer Ayed, 2018). Recent research indicates that approximately 69% of total groundwater withdrawals are linked to agricultural activities, 22% to industrial usage, 8% to domestic consumption, and 1% to recreational purposes (Rosegrant et al., 2009). Groundwater contamination primarily stems from wastewater discharge, notably from industries, as well as effluents from human settlements, improper hazardous waste disposal, and pollution from agricultural areas and roads (Ivana Ilić, 2021., Chandrasekar V et al., 2017., Shanmugasundharam et al., 2015).

Groundwater stands as a valuable natural asset, with environmental challenges varying based on geological, hydrological, climatic conditions, and geochemical factors unique to each region.

Water quality degradation can be broadly categorized into two types: those resulting from natural conditions and those stemming from human activities. (Nitasha Khatri, 2014). The extraction or alteration of recharge patterns can modify groundwater flow directions or expose aquifer materials to air, potentially leading to the encounter of clean water with natural contaminants such as radium, salt, arsenic, and fluoride, thereby affecting water quality and causing associated health concerns. Furthermore, chemical and biological contaminants originating from industrial and agricultural sources further deteriorate water quality (Abhay Kumar Soni, 2019).

All groundwater contains minerals dissolved in solution, with the type and concentration of these minerals depend on various factors, such as surface and subsurface environment, groundwater flow rates, and the groundwater source (Jasechko, S, 2024). When precipitation interacts with different soil constituents, it is relatively mineral-free. However, due to water's solvent properties, minerals dissolve and become part of the groundwater as it percolates through the aquifer (Venkateswaran, 2015). The concentrations of cations and anions in groundwater rely on the solubility of minerals in geological formations, the duration of contact with rocks, and the level of dissolved CO₂ in the water (Ali, M., et.al, 2022). Chemical alterations in groundwater are influenced by various factors, including interactions with solid phases, groundwater residence time, mixing with saline water pockets, and anthropogenic influences (Stallard, 1983). The quality of groundwater quality is also affected by seawater intrusion in coastal areas which is a natural process. However human exploitation of coastal aquifers exacerbates the issue (Prusty, P et.al., 2020). Besides natural salinity, anthropogenic activities significantly contribute to the deterioration of water quality (Egun, 2010). Therefore, the study aims to assess the quality of coastal groundwater and the spatial distribution of various hydrogeochemical parameters to determine the suitability of groundwater resources in Ponneri and Thiruvottriyur taluk in Northern Coast of Tamil Nadu, which is densely populated and heavily rely on groundwater for domestic and agricultural purposes.

Study Area

Ponneri taluk is situated in the Tiruvallur district of the Indian state of Tamil Nadu, which covers an area of 674 sq.km (Figure 1a). With an average elevation of 16 meters (52 feet), Ponneri serves as the administrative centre of the taluk. As per the 2011 census, Ponneri taluk had a population of 3,85,620, comprising 1,93,043 males and 1,92,577 females (Census of India, 2011). Tiruvottriyur is a small coastal taluk esplanade nestled along the Bay of Bengal coast. Historically, sea encroachment posed significant challenges for local fishermen until the construction of groynes commenced in 2004. Spanning over 4 kilometres, these groynes vary in length from 165 to 300 meters each and stand at a height of four meters above mean sea level. Over time, several acres have been reclaimed with the formation of a beach, aligning with earlier predictions.

Table 1. List of Villages (Sample collection site)

S.No	Village	S.No	Village
1	Annaimalaicherry	20	Kodipalam
2	Arasur	21	Kodur
3	Attipattu Pudu Nagar	22	Kuruviagaram
4	Attur	23	New Manali Town
5	Chellappa Nagar	24	Orukaddu
6	Edapalayam	25	Pazhaverkadu
7	Ennore Burma Nagar	26	Penchetty
8	Gounderpalayam	27	Pudupet
9	Illupakkam	28	Puduvoyal
10	Indira Gandhi Colony	29	Telugu Colony
11	Jyothi Nagar	30	Thathaimanji
12	Kadapakkam	31	Thirupallivanam
13	Kalanji	32	Thiruvellavoyal
14	Kaniyambakkam	33	Ooplibedu
15	Kumanoor	34	Vanichatram
16	Karumariamman Nagar	35	Vepathoor
17	Kattavur	36	Vettukuppam
18	Kesvapuram	37	Vichoor
19	Kilmuldalaibedu		

The sodium (Na⁺) and potassium (K⁺) content in groundwater were estimated using an EEL flame photometer equipped with a proper Air-LPG flame, with sodium and potassium sulphate standards of appropriate concentrations being utilized. All parameters are expressed in milligrams per liter (mg/l), except for pH (no units) and electrical conductivity (EC) is reported in microsiemens per centimeter ($\mu\text{S/cm}$) at 25°C.

GIS Modelling

GIS has emerged as a potent tool for generating spatial distribution maps, offering insights into the variation in concentrations of various chemical parameters. These maps were prepared using the inverse distance weighted (IDW) raster interpolation technique within the spatial analyst module of ArcGIS (Shanmugasundharam, 2015; Chandrasekar V, 2017). The accuracy of results obtained through IDW interpolation is contingent upon the density and distribution of the sampling points relative to the local variations being modelled. Sparse or uneven sampling may compromise the fidelity of the results, failing to adequately capture the desired surface characteristics.

In the inverse distance weighted (IDW) interpolation method, the predicted value Z_p at location S_0 is calculated using the formula

$$Z_p = \sum_{i=1}^n \left(\frac{z_i}{dip} \right) / \sum_{i=1}^n \left(\frac{1}{dip} \right)$$

Where, n represents the number of measured sample points surrounding the prediction location that is used in the prediction, z_i denotes the observed value at location

, and *dip* signifies the distance between the prediction location *S0* and the measured sample location *Si*. The weights assigned to each measured point are inversely proportional to the distance, meaning closer points have more influence on the predicted value. Among several interpolation techniques compared in this study, IDW with a squared distance term yielded more consistent results. Consequently, spatial distribution maps were generated for selected water quality parameters, including pH, TDS, TH, total alkalinity, chloride, nitrates, fluoride, Ca^{2+} , Mg^{2+} , and Water Quality Index (WQI) (D. Janardhana Rao, 2016).

Multivariate Statistical Analysis and Graphical Representation

Various statistical methods and graphs were employed to substantiate the deterioration of groundwater quality. Piper trilinear plots was utilized for hydro-chemical classification. Hierarchical Cluster Analysis (HCA) assessed water chemical profiles, ensuring data accuracy and identifying correlations. A correlation matrix computed R-values, indicating the degree of linear association between parameters. R ranges from -1 to +1, with +1 or close indicating a strong positive correlation, and -1 or close revealing a strong negative correlation, highlighting interrelated parameters influencing water quality in the area. The Gibb's ratio methodology is a hydrogeochemical technique used to assess water composition and understand the processes impacting aquifer systems. It involves calculating ratios of major ions like Na^+/K^+ , Na^+/Cl^- , and Ca^{2+} . These ratios help identify dominant processes such as evaporation, rock-water interaction, or precipitation affecting water chemistry. By comparing these ratios with theoretical values associated with specific hydro geochemical processes.

Result and Discussion

The physicochemical parameters of groundwater samples were analyzed, and the descriptive statistics of the analyzed parameters are presented in Table 2. These results are compared with the standard values set by the World Health Organization and the Bureau of Indian Standards (BIS).

Table 2. Comparison of analytical results with international and national standards

Parameters	Post-Monsoon		Pre-Monsoon		Mean		WHO Guidelines (2004)	BIS Guidelines (2012)
	Max	Min	Max	Min	Post-Monsoon	Pre-Monsoon		
EC ($\mu\text{s}/\text{cm}$)	8370	400	7790	490	2584.32	2546.41	1500	-
pH	7.3	5.8	7.8	5.8	6.81	6.97	6.5 - 8.5	6.5 – 8.5
TDS	4191	212	4340	250	1417.54	1440.88	1500	500 – 2000
Ca	384	34	460	32	129.02	128.14	200	75 – 200
Mg	316	19	233	10	63.27	68.46	150	-
Na	1051	12	807	12	314.45	296.93	200	200 – 400
K	227	0	74	0	20.05	20.87	12	-
Cl	2233	46	2233	67	509.86	539.31	600	250
SO ₄	668	14	1094	7	153.73	163.97	250	200 – 400
NO ₃	256	0	549	0	43.51	57.69	-	45
F	1.7	0	1.1	0.01	0.36	0.41	1.5	1.0 – 1.5

pH

The data presented in Table No. 2 illustrates that the pH of groundwater ranged from 5.8 to 7.3 during the post-monsoon period, with an average value of 6.81, indicating nearly neutral conditions. In the pre-monsoon period, pH values ranged from 5.8 to 7.8, with a mean value of 6.97, also indicating neutral conditions in the coastal regions. The lowest post-monsoon pH values were recorded in Vanichatram and Attur villages with 5.8 and 6.2, respectively, indicating acidity. Vepathoor recorded the highest post-monsoon, pH level at 7.3. Approximately, 94.5% of water samples fall within the permissible pH range for drinking, according to BIS 2012, which is 6.5–8.5 (IS: 10500-1991). Most of the samples fall within this range. Similarly, during the pre-monsoon period, Vanichatram village recorded the lowest pH level at 5.8, while Pazhaverkadu recorded the highest pH level at 7.8. Only one sample (Pazhaverkadu) in the northern part exhibited moderately alkaline water, while three samples with an acidic nature were found in the southwestern part of the study area (Figure 2a).

Electrical Conductivity

In the post-monsoon period, the electrical conductivity ranged from 400 to 8370 $\mu\text{S}/\text{cm}$, with an average value of 2584.32 $\mu\text{S}/\text{cm}$ (Table 2). The lowest recorded value was observed in Attur village, situated in the western part of the study area. It's worth noting that this village is located above the Cholavaram Tanks. Due to this, water contamination is very low and the aquifer is quickly recharged. In the study area, during the post-monsoon period, the highest electrical conductivity (EC) levels were observed in the eastern and southeastern parts. Karumariamman Nagar recorded the highest EC level at 8370 $\mu\text{S}/\text{cm}$, situated adjacent to the industrial area. This region experiences significant water extraction activities, especially due to the presence of Ennore port and North Chennai Thermal Power station, impacting both the region and the livelihoods of many farmers and anglers (Figure 2b). Approximately, 30% of the water samples exceeded the permissible limit (above 3000 $\mu\text{S}/\text{cm}$) and are deemed unfit for drinking. Only 16% of the study area exhibited EC levels below the acceptance limit, including Pudevoyal, Vanichatram, and Kilmuldalaibedu. These villages are situated away from coastal and industrial regions and are surrounded by numerous tanks. In the pre-monsoon period, Attur village recorded a low EC level of 490 $\mu\text{S}/\text{cm}$, while Karumariamman Nagar recorded 7790 $\mu\text{S}/\text{cm}$. Around 30% of the samples exhibited high EC levels near Ennore Port and Thermal Station, affecting the southern and eastern parts of the study area. Groundwater near these regions is highly contaminated, resembling saltwater, with many wells showing yellowish water. Agricultural production has been significantly impacted due to water contamination. The spatial distribution of EC values depicted in Figure 3 indicates an increase from east to west, implying the direction of flow. The significant variations in EC are primarily attributed to anthropogenic activities and prevailing geochemical processes in the region. EC typically increases along groundwater flow paths due to the combined effects of evaporation, ion exchange, and topographic conditions

Total Dissolved Solids

In the post-monsoon period, the TDS levels ranged from 212 to 4191 mg/l (Table 2). The lowest recorded value was observed in Attur Village, situated in the western part of the study area. This village is positioned above the Cholavaram Tanks, resulting in significant water contamination but rapid aquifer recharge. The highest TDS levels were recorded in the eastern and southeastern parts of the study area, with Karumariamman Nagar registering the highest TDS level at 4191 mg/l (Figure 2c), and this village is located adjacent to the industrial area (Figure.1b). In the pre-monsoon period, data collected in July indicated higher water contamination levels compared to the post-monsoon period. The TDS levels during pre-monsoon ranged from 250 to 4340 mg/l. Attur village exhibited the lowest TDS levels at 250 mg/l, while Karumariamman Nagar recorded the highest TDS level at 4340 mg/l. Approximately, 21.6% of the samples exhibited high TDS levels near Ennore Port and Thermal Station, highlight the significant impact of industrial activities and geomorphological settings on groundwater quality

Calcium

In the post-monsoon season, calcium concentration levels ranged between 34 and 384 mg/l. The lowest calcium concentration was recorded in Puduvoiyal and Attur villages, located in the western part of the study area (Figure 2d). Cholavaram tanks situated below Attur village contribute to the natural recharge of aquifers, thereby reducing contamination levels. The highest Ca^{2+} level was observed in the central and eastern parts of the study area. During the pre-monsoon season, calcium levels ranged from 32 to 460 mg/l. Puduvoiyal village exhibited the lowest Ca^{2+} level at 32 mg/l, while Karumariamman Nagar recorded the highest Ca^{2+} level at 460 mg/l. Approximately, 16% of the samples collected near Ennore Port and Thermal Station showed high Ca^{2+} levels, indicating saline groundwater. The significant calcium levels near Ennore Port and Thermal Station indicate localized saline groundwater contamination, emphasizing the need for targeted monitoring and remediation efforts.

Magnesium

In the post-monsoon season, Mg^{2+} levels ranged from 19 to 316 mg/l. The lowest magnesium level was recorded in Attur village, situated in the southwestern part of the study area. The highest Mg^{2+} level was observed in the eastern part of the study area, specifically in Karumariamman Nagar at 316 mg/l, attributed to high water extraction activities (Figure 3a). Only 3 samples exceeded the permissible limit, rendering them unfit for drinking. During the pre-monsoon season, magnesium levels ranged from 10 to 233 mg/l. Attur village displayed the lowest Mg^{2+} level at 10 mg/l, while the highest magnesium level was found in New Manali Town at 233 mg/l. indicate the impact of high-water extraction activities and industrial influences on groundwater quality. The presence of elevated magnesium levels in specific areas underscores the need for targeted water management and monitoring strategies to ensure safe drinking water.

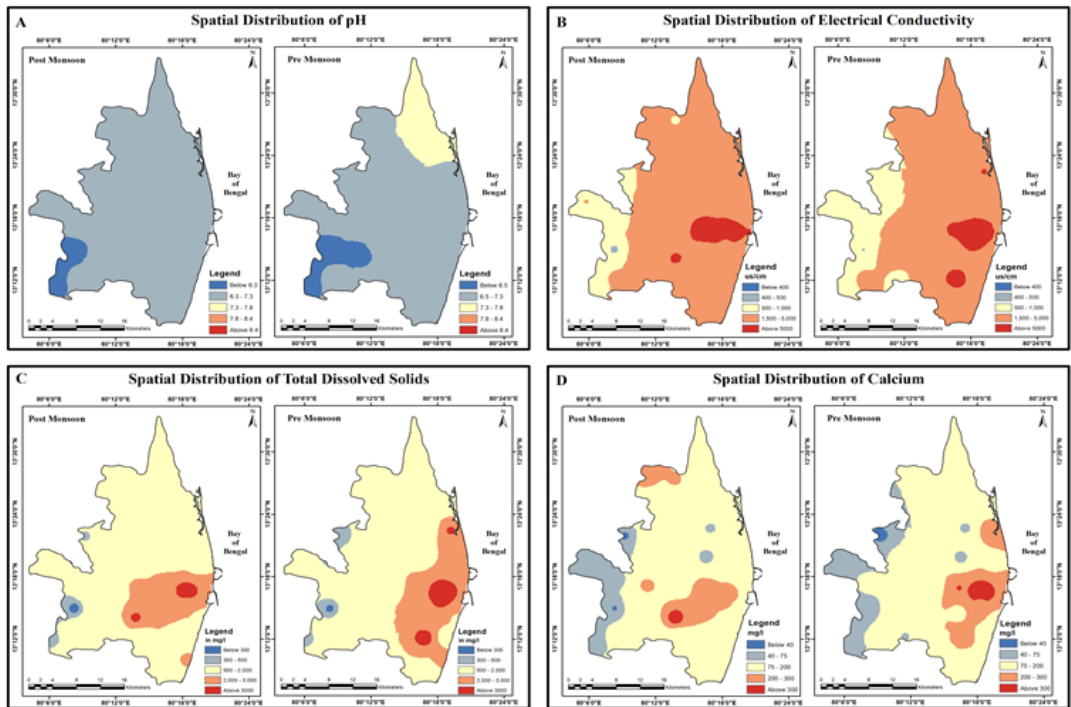


Figure 2. Spatial Distribution of Water Quality Parameters (pH, EC, TDS, Ca²⁺) Sodium

In the post-monsoon season Figure 3b, the Na⁺ levels ranged from 12 to 1051 mg/l (Table 2). The lowest recorded Na⁺ value was observed in Attur Village, situated above the Cholavaram Tanks in the southwestern part of the study area. Conversely, the highest Na⁺ level was observed across various parts of the study area, with Karumariamman Nagar recording the highest Na⁺ level at 1051 mg/l. This village is adjacent to the industrial area, rendering it susceptible to high contamination levels. Approximately, 70% of water samples exceeded permissible limits, rendering them unfit for drinking according to World Health Organization standards (WHO, 2004). During the pre-monsoon season, data collected in July revealed sodium (Na⁺) levels ranging from 32 to 807 mg/l. Attur village exhibited the lowest sodium level at 32 mg/l, while Karumariamman Nagar recorded the highest level at 807 mg/l. Approximately, 46% of the samples exhibited high Na⁺ levels, primarily concentrated near the Ennore Port and Thermal Station.

Potassium

In the post-monsoon season, the K⁺ levels ranged from 0 to 227 mg/l (Table 2). The lowest values were recorded in 21 villages, primarily located in the southern part of the study area. The villages with low potassium levels are situated in the western region, characterized by lesser water contamination and abundant lakes and tanks, leading to rapid aquifer recharge. The highest K⁺ levels were observed in the eastern part of the study area

(Figure 3c). Pudupet recorded the highest potassium level at 227 mg/l, while Vichoor recorded 203 mg/l. These villages are located adjacent to industrial areas, where water extraction rates are notably high. Approximately 32% of water samples exceeded permissible limits, rendering them unsuitable for drinking. Comparatively, water contamination levels were higher during the pre-monsoon period. During the pre-monsoon season, potassium levels ranged from 0 to 74 mg/l. Seven villages and Kadapakkam exhibited low potassium levels, with Kadapakkam recording 74 mg/l. The presence of high potassium levels exceeding permissible limits in 32% of samples indicates an urgent need for enhanced groundwater management and pollution control measures to protect water resources.

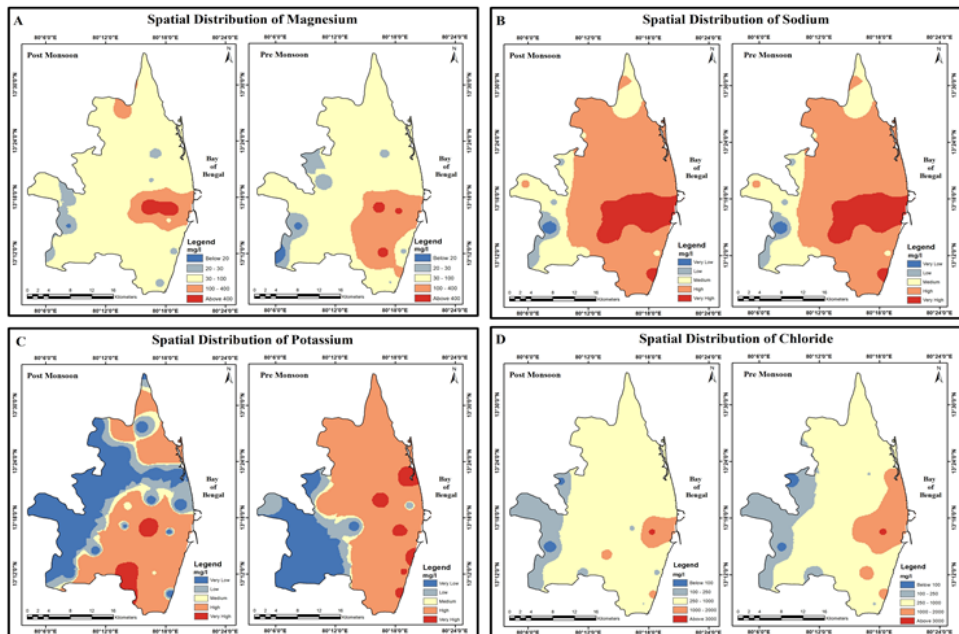


Figure 3. Spatial Distribution of Water Quality Parameters (Mg^{2+} , Na^+ , K^+ , Cl^-) Chloride

In the post monsoon season, the concentration of chloride ranged from 46 to 2233 mg/l. The lowest values of Cl^- concentration were recorded in Attur and Puduvoiyal Villages, with 46 and 60 mg/l, respectively. Conversely, the highest Cl^- level was observed in the eastern part of the study area (Figure 3d), with Karumariamman Nagar recording the highest Cl^- level at 2233 mg/l. Data collected during the pre-monsoon period in July, when water contamination levels are comparatively high, revealed Cl^- concentration levels ranging from 67 to 2233 mg/l. Attur village exhibited the lowest Cl^- levels at 67 mg/l, while Karumariamman Nagar recorded the highest Cl^- level at 2233 mg/l. The consistently high chloride levels in Karumariamman Nagar emphasize the critical impact of industrial activities and the necessity for rigorous groundwater monitoring and effective pollution mitigation strategies.

Piper Diagram:

The graphical representation of Piper's diagram (Figure 4) illustrates that the majority of water samples cluster within the Na-Cl field, resembling seawater characteristics, indicating a prevalence of sodium and chloride ions. However, there are a few stations that fall into the mixed Ca-Mg field. This distribution on the Piper diagram underscores those alkalis (Na^+ and K^+) exceed alkaline earth elements (Ca^{2+} and Mg^{2+}), and chloride predominates over other anions in the water samples. This analysis provides valuable insights into the chemical composition and characteristics of the groundwater samples, emphasizing the dominance of specific ions and the prevailing chemical patterns.

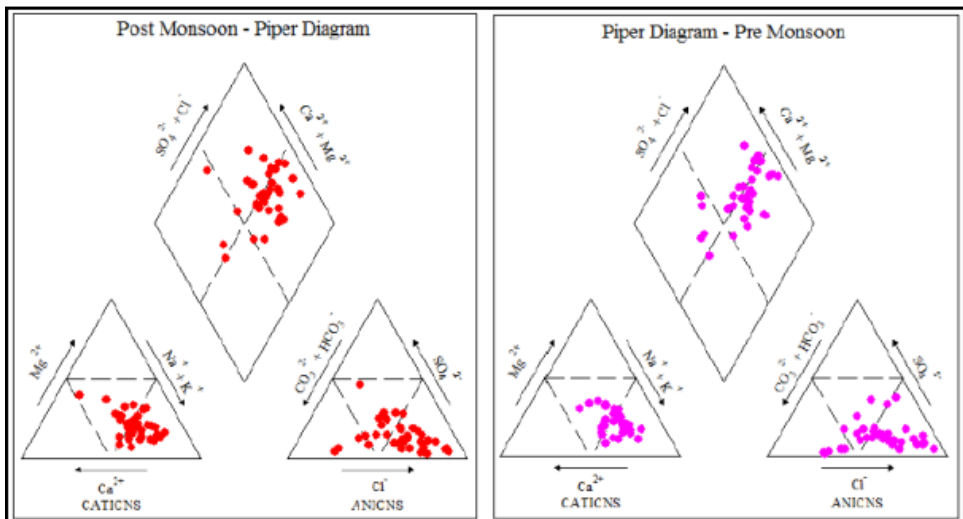


Figure 4. Piper diagram displaying the hydrological facies of the samples
Multivariate Statistical Analysis for the Groundwater

Post-Monsoon Correlation

During the post-monsoon period (Figure 5), a strong positive correlation is observed between EC and TDS, indicating that as EC increases, and TDS levels also tend to rise. This correlation extends to sodium (Na^+), magnesium (Mg^{2+}), and calcium carbonate (CaCO_3), suggesting a common origin or shared influence among these elements. Furthermore, strong correlations are noted between Mg-Na, Na-Cl, and Mg-Cl, implying a common source or similar geochemical processes affecting these elements. Moderate correlations are also observed among calcium (Ca^{2+}), bicarbonate (HCO_3^-), sulphate (SO_4^{2-}), chloride (Cl^-), and total alkalinity, indicating potential associations or shared origins among these parameters. Conversely, weaker correlations are found with fluoride (F^-), nitrate (NO_3^-), and potassium (K^+), suggesting less pronounced relationships or diverse sources for these elements. In terms of interdependencies, moderate correlations are observed between Ca-Na, Ca- SO_4 , Mg-Cl, Cl-Ca, and Cl-Mg, indicating potential interactions or influences among these pairs of elements. However, weaker correlations are

noted between EC-K, EC-F, EC-NO₃, Ca-Mg, Ca-K, Ca-NO₃, Mg-K, Mg-NO₃, Mg-F, Na-K, and K-SO₄, suggesting less significant relationships or varying sources for these particular combinations of elements. These weaker correlations may reflect the influence of diverse sources or geochemical processes on these elements during the post-monsoon period.

Pre- Monsoon Correlation

During the pre-monsoon (Figure 5) period, strong positive correlations are observed between EC and TDS with calcium (Ca²⁺), magnesium (Mg²⁺), sodium (Na⁺), chloride (Cl⁻), and calcium carbonate (CaCO₃), indicating that these ions significantly contribute to TDS levels and play crucial roles in water quality. The strong correlations between TDS and major ions such as Na⁺, Mg²⁺, Ca²⁺, Cl⁻, and SO₄²⁻ further suggest their predominant contribution to increased TDS levels. The robust correlations between major ions and both EC and TDS underscore that these ions are primary factors influencing water electrical conductivity and total dissolved solids. Factors contributing to these correlations may include evaporation, rock-water interactions, and silicate weathering processes. Moderate correlations are identified among various ion pairs, including Ca-K, Mg-SO₄, Na-K, Na-SO₄, K-Na, K-Cl, NO₃, and Cl-K. Additionally, moderate correlations are observed between Ca-HCO₃, Ca-SO₄, Ca-NO₃, Mg-K, Mg-HCO₃, Mg-NO₃, Cl-HCO₃, Cl-SO₄, Cl-NO₃, Na-HCO₃, Na-NO₃, K-Ca, K-Mg, and K-SO₄. Weak correlations are noted between fluoride and various ions, with some values indicating negative correlations, suggesting potential complex interactions. The prevalence of low correlations with NO₃⁻ implies diverse influences on this ion, while fluoride exhibits numerous negative correlations with other ions. Overall, the observed correlations highlight the complex interplay among various ions and factors influencing groundwater chemistry during the pre-monsoon period.

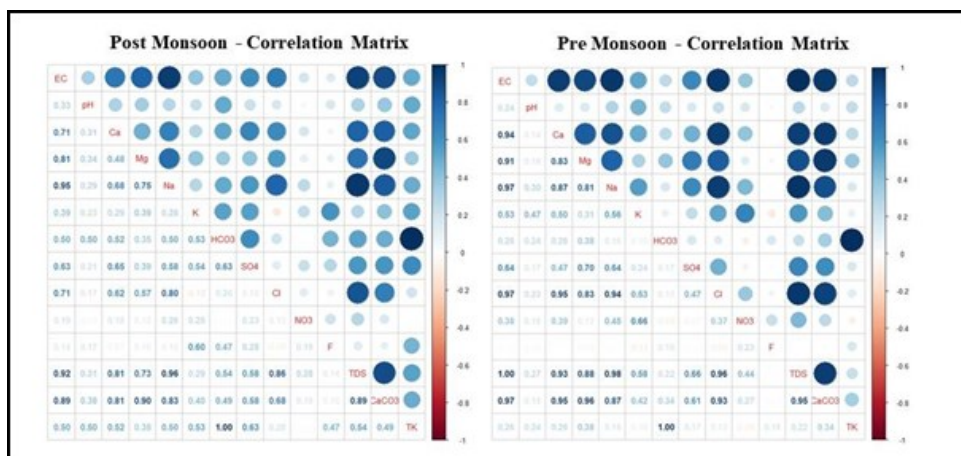


Figure 5. Post and Pre- Monsoon Correlation Matrix

Gibbs Ratio

The Gibbs diagram is commonly employed to validate the connection between water composition and aquifer lithological traits, delineating three distinct fields: evaporation

dominance, rock-water interaction dominance, and precipitation dominance. In post-monsoon (2017), the predominant samples fall in the evaporation dominance and rock water Interaction field of the Gibbs diagram (Figure 6a). The area under rock–water interaction dominance field indicates the interaction between rock chemistry and the chemistry of the percolated waters under the subsurface. In pre-monsoon (2017), figure 6b, the predominant samples fall in the evaporation dominance and Rock water Interaction field of the Gibbs diagram. This plot explains the relationship between water chemistry and aquifer lithology. Such a relationship helps to identify the factors controlling the groundwater chemistry

$$\text{Gibbs Ratio (I) (For Cations): } (Na^{+}+K^{+})/(Na^{+}+K^{+}+Ca^{2+}) \quad \text{Eq - 1}$$

$$\text{Gibbs Ratio (II) (For Anions): } Cl^{-}/(Cl^{-}+HCO_3^{-}) \quad \text{Eq – 2}$$

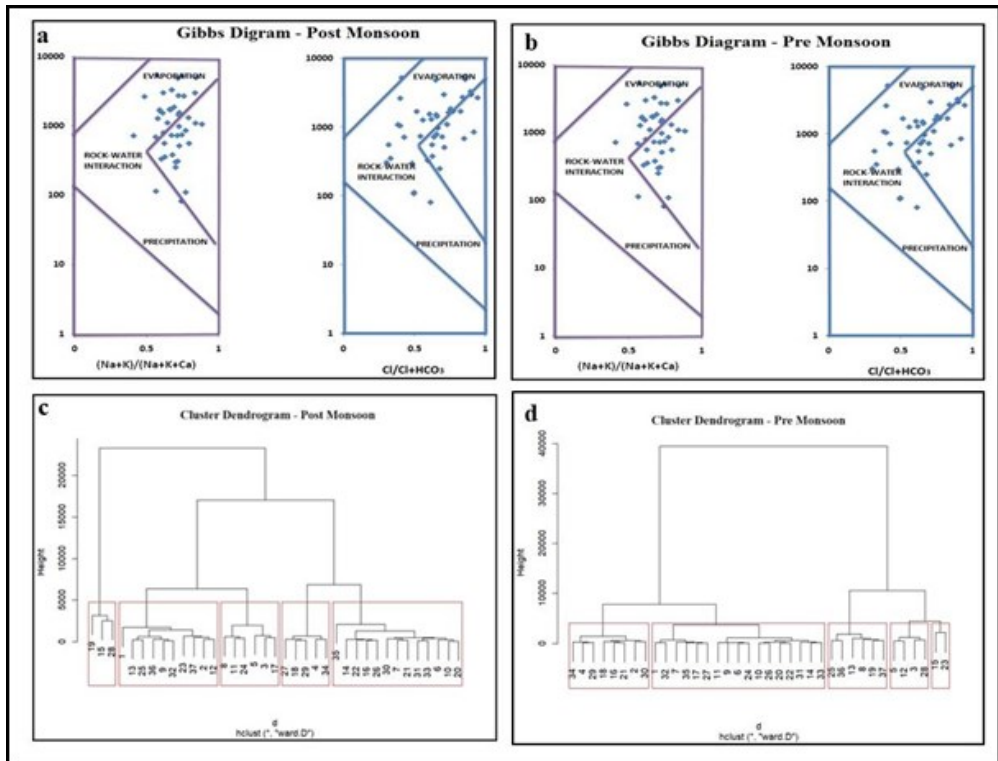


Figure 6. Gibbs Ratio and Cluster Dendrogram of Water Quality
Hierarchical cluster analysis (HCA)

In the current study, cluster analysis has been instrumental in revealing groups of sampled stations sharing similarities, generating a dendrogram using the ward method for both post-monsoon and pre-monsoon periods. In the post-monsoon analysis (Fig. No. 6c), the dendrogram effectively delineates five statistically significant clusters from the 37

sampling stations. The initial cluster encompasses three locations (19, 15, 28), the second cluster comprises samples from 10 locations (13, 25, 36, 9, 32, 23, 37, 2, and 12), the third cluster includes six samples (8, 11, 24, 5, 3, and 17), and the fourth cluster includes five samples (27, 18, 29, 4, and 34), while the remaining samples collectively form the fifth and final cluster with 13 samples. This hierarchical clustering approach enables meaningful categorization of water samples based on their hydrogeochemical characteristics, with differences reflecting variations in morphology and anthropogenic pollution. Notably, sampling sites under clusters 4 and 5, located in commercial and coastal areas, exhibit extensive human activity and water source pollution.

Similarly, in the pre-monsoon analysis (Fig. No. 6d), the hierarchical clustering approach categorizes water samples into distinct groups. The initial cluster encompasses eight locations (34, 4, 29, 18, 16, 21, 2, and 30), the second cluster comprises samples from 17 locations (1, 32, 7, 35, 17, 27, 11, 9, 6, 24, 10, 26, 20, 22, 31, 14, 33), the third cluster includes six samples (25, 36, 13, 8, 19, 37), the fourth cluster includes four samples (5, 12, 3, 28), while the remaining samples collectively form the fifth and final cluster with two samples. Again, sampling sites under clusters 4 and 5, situated in commercial and coastal areas, exhibit significant human activity and water source pollution.

Conclusion

The study highlights significant physicochemical variations in groundwater quality in Ponneri and Tiruvottriyur taluks of Tiruvallur district. Anthropogenic activities, particularly industrialization and urbanization, contribute to elevated pH, electrical conductivity, and total dissolved solids, impacting water suitability. The spatial distribution reveals localized contamination near industrial zones, affecting aquifers and livelihoods. Sodium and potassium levels exceed permissible limits in certain areas, nearly 51% locations are unsuitable for drinking.

The hydrogeochemical analysis of groundwater samples, illustrated through Piper-trilinear plots, multivariate statistical analysis, and hierarchical cluster analysis, provides a comprehensive understanding of the complex interactions and variations in water quality. The Piper diagram emphasizes the prevalence of Na-Cl characteristics in most samples. The multivariate analysis reveals strong correlations among various ions, indicating shared origins or geochemical processes. The area under rock-water interaction dominance field indicates the interaction between rock chemistry and the chemistry of the percolated waters under the subsurface. Hierarchical cluster analysis effectively categorizes sampling stations based on hydrogeochemical characteristics, emphasizing the impact of anthropogenic activities and environmental factors on groundwater quality during both post-monsoon and pre-monsoon periods.

Declaration

It is declared that the manuscript submitting to IGS journal is original work of the author(s) and it is not published already or submitted elsewhere for publication.

References

1. Soni, A. K. (2019). Mining of Minerals and Groundwater in India. *Groundwater - Resource Characterisation and Management Aspects*. DOI: 10.5772/intechopen.85309
2. Ali, M., Jha, N. K., Pal, N., Keshavarz, A., Hoteit, H., & Sarmadivaleh, M. (2022). Recent advances in carbon dioxide geological storage, experimental procedures, influencing parameters, and future outlook. *Earth-Science Reviews*, 225, 103895.
3. APHA (1989). Standard methods for the examination of water and wastewater, 17th ed. Washington, DC, *American Public Health Association*.
4. Atlas U (2010). Atlas U.N.: 44 Percent of us live in Coastal Areas. <http://coastalchallenges.com/2010/01/31/un-atlas-60-of-us-live-in-thecoastalareas/>
5. Ayed, B., Jmal, I., Sahal, S., & Bouri, S. (2018). The seawater intrusion assessment in coastal aquifers using GALDIT method and groundwater quality index: the Djefara of Medenine coastal aquifer (Southeastern Tunisia). *Arabian Journal of Geosciences*, 11, 609. <https://doi.org/10.1007/s12517-018-3966-8>
6. Boukari, M., Gaye, C. B., Faye, A., & Faye, S. (1996). The impact of urban development on coastal aquifers near Cotonou, Benin. *J Afr Earth Sci*, 22(4), 403–408.
7. Census of India (2011). Provisional Population Totals - Tamil Nadu-Census 2011 Sub District (Taluk) Level.
8. Chandrasekar, V., Shaik, M., & Ravikumar, P. (2017). An Assessment of Groundwater Quality in Coastal Taluks of Tiruvallur Districts in Tamil Nadu, India. *International Journal for Research in Applied Science & Engineering Technology*, 5(8).
9. Chilton, J. (1996). Water Quality Assessments - A Guide to Use of Biota, Sediments and Water in Environmental Monitoring - Second Edition. Chapter 9 *Groundwater*. Edited by Deborah Chapman.
10. Igbah, C. E., & Tanko, J. A. (2019). Assessment of urban groundwater quality using Piper trilinear and multivariate techniques: a case study in the Abuja, North-central, Nigeria. *Environmental Systems Research*.
11. Egun, N. K. (2010). Effect of channelling wastewater into water bodies: a case study of the Orogodo River in Agbor, Delta State. *J Hum Ecol*, 31(1), 47–52.
12. Foppen, J. W. A. (2002). Impact of high-strength wastewater infiltration on groundwater quality and drinking water supply: the case of Sana'a, Yemen. *J Hydrol*, 263, 198–216.
13. Ilić, I., Puharić, M., & Ilić, D. (2021). Groundwater Quality Assessment and Prediction of Spatial Variations in the Area of the Danube River Basin (Serbia). *Water Air Soil Pollution*, 232, 117. <https://doi.org/10.1007/s11270-021-05069-4>
14. Jasechko, S., Seybold, H., Perrone, D., et al. (2024). Rapid groundwater decline and some cases of recovery in aquifers globally. *Nature*, 625, 715–721. <https://doi.org/10.1038/s41586-023-06879-8>
15. Adimalla, N., Dhakate, R., Kasarla, A., & Taloor, A. K. (2020). Appraisal of groundwater quality for drinking and irrigation purposes in Central Telangana, India. *Groundwater for Sustainable Development*, 10. <https://doi.org/10.1016/j.gsd.2020.100334>
16. Adimalla, N., & Venkatayogi, S. (2018). Geochemical characterization and evaluation of groundwater suitability for domestic and agricultural utility in semi-arid region of Basara,

- Telangana State, South India. *Applied Water Science*, 8, 44. <https://doi.org/10.1007/s13201-018-0682-1>
17. Khatri, N., & Tyagi, S. (2014). Influences of natural and anthropogenic factors on surface and groundwater quality in rural and urban areas. *Frontiers in Life Science*, 8(1). <https://doi.org/10.1080/21553769.2014.933716>
 18. Prasad, B., Rao, P. R., & Tigga, A. (2021). Groundwater quality assessment using the weighted arithmetic index method in the selected villages of Butchayyapeta Mandal, Visakhapatnam, Andhra Pradesh, India. *Environmental Monitoring and Assessment*, 193, 1-17.
 19. Prusty, P., & Farooq, S. H. (2020). Seawater intrusion in the coastal aquifers of India-A review. *HydroResearch*, 3, 61-74.
 20. Silva-Madera, R. J., Salazar-Flores, J., Peregrina-Lucano, A. A., Mendoza-Michel, J., Ceja-Gálvez, H. R., Rojas-Bravo, D., Reyna-Villela, M. Z., & Torres-Sánchez, E. D. (2021). *Water Air Soil Pollution*, 232, 43.
 21. Rosegrant, M. W., Ringler, C., & Zhu, T. (2009). Water for agriculture: maintaining food security under growing scarcity. *Annu Rev Environ Resour*, 34(1), 205–222. <https://doi.org/10.1146/annurev.envir>
 22. Shanmugasundharam, G., Kalpana, S. R. M., Sudharson, E. R., & Jayaprakash, M. (2015). Assessment of Groundwater quality in Krishnagiri and Vellore Districts in Tamil Nadu, India. *Applied Water Science*, 7, 1869–1879.
 23. Stallard, R. F., & Edmond, J. M. (1983). Geochemistry of the Amazon River. The influence of the geology and weathering environment on the dissolved load. *J Geophys Res*, 88, 9671-9688.
 24. Steinhorst, R. K., & Williams, R. E. (1985). Discrimination of groundwater sources using cluster analysis, MANOVA, canonical analysis and discriminant analysis. *Water Resour Res*, 21, 1149–1156.
 25. Subba Rao, N. (2006). Seasonal variation of groundwater quality in a part of Guntur District, Andhra Pradesh, India. *Environ Geol*, 49, 413–429.
 26. Venkateswarana, S., & Deepa, S. (2015). Assessment of Groundwater Quality using GIS Techniques in Vaniyar Watershed, Ponnaiyar River, Tamil Nadu. *Aquatic Procedia*, 4, 1283–1290. doi: 10.1016/j.aqpro.2015.02.167
 27. World Health Organization (WHO) (2011). Guidelines for drinking water quality, 4th edn. *World Health Organization*, Geneva.